NeuroImage 159 (2017) 248–260

Contents lists available at ScienceDirect

NeuroImage

journal homepage: www.elsevier.com/locate/neuroimage

Frequency-specific modulation of connectivity in the ipsilateral sensorimotor cortex by different forms of movement initiation

Bin A. Wang [a], Shivakumar Viswanathan [a,b], Rouhollah O. Abdollahi [a], Nils Rosjat [a,c], Svitlana Popovych [a,c], Silvia Daun [a,c], Christian Grefkes [a,b], Gereon R. Fink [a,b,*]

[a] Cognitive Neuroscience, Institute of Neuroscience and Medicine (INM-3), Research Centre Jülich, 52425, Jülich, Germany
[b] Department of Neurology, University Hospital Cologne, 50924, Cologne, Germany
[c] Heisenberg Research Group of Computational Neuroscience - Modeling Neural Network Function, Department of Animal Physiology, Institute of Zoology, University of Cologne, 50674, Cologne, Germany

ARTICLE INFO

Keywords:
Event-related spectral perturbation (ERSP)
Coherence
Ipsilateral activity
Self-initiated
Visually-cued

ABSTRACT

A consistent finding in motor EEG research is a bilateral attenuation of oscillatory activity over sensorimotor regions close to the onset of an upcoming unilateral hand movement. In contrast, little is known about how movement initiation affects oscillatory activity, especially in the hemisphere ipsilateral to the moving hand. We here investigated the neural mechanisms modulating oscillatory activity in the ipsilateral motor cortex prior to movement onset under the control of two different initiating networks, namely, *Self-initiated* and *Visually-cued* actions. During motor preparation, a contralateral preponderance of power over sensorimotor cortex (SM) was observed in α and β bands during *Visually-cued* movements, whereas power changes were more bilateral during *Self-initiated* movements. Coherence between ipsilateral SM (iSM) and contralateral SM (cSM) in the α-band was significantly increased compared to the respective baseline values, independent of the context of movement initiation. However, this context-independent cSM-iSM coherence modulated the power changes in iSM in a context-dependent manner, that is, a stronger cSM-iSM coherence correlated with a larger decrease in high-β power over iSM in the *Self-initiated* condition, in contrast to a smaller decrease in α power in the *Visually-cued* condition. In addition, the context-dependent coherence between SMA and iSM in the α-band and δ-θ-band for the *Self-initiated* and *Visually-cued* condition, respectively, exhibited a similar context-dependent modulation for power changes. Our findings suggest that the initiation of regional oscillations over iSM reflects changes in the information flow with the contralateral sensorimotor and premotor areas dependent upon the context of movement initiation. Importantly, the interaction between regional oscillations and network-like oscillatory couplings indicates different frequency-specific inhibitory mechanisms that modulate the activity in the ipsilateral sensorimotor cortex dependent upon how the movement is initiated.

1. Introduction

During movement preparation and execution, oscillatory power over the sensorimotor regions (measured by electroencephalography (EEG)) typically shows an attenuation both in the α-band (8–13 Hz) and the β-band (13–30 Hz), a phenomenon known as event-related desynchronization (ERD) (Meirovitch et al., 2015; Notturno et al., 2014; Pfurtscheller, 1989, 1981; Pfurtscheller et al., 2006). Prior to unilateral hand movements, ERD is not only detected over the contralateral (cSM) but also over the ipsilateral sensorimotor cortex (iSM) (Bai et al., 2005; Pfurtscheller and Lopes Da Silva, 1999; Szurhaj et al., 2001). In the current study, using EEG we investigated the network basis of ERD over the iSM modulated by different movement initiation contexts.

The ERD ipsilateral to the moving hand has been shown to be modulated by a number of different movement contexts. For example, increasing movement complexity is associated with a concurrent increase of ipsilateral activity in the α-band (Chen et al., 1997; Hummel et al., 2003; Manganotti et al., 1998; Tinazzi and Zanette, 1998). Van Wijk et al. (2012) reported that β-band ERD occurred during continuous dynamic but not during static force production, suggesting that activity in ipsilateral primary motor cortex is relevant for the accurate timing of movement sequences but not maintenance. Furthermore, Rossiter et al.

* Corresponding author. Cognitive Neuroscience, Institute of Neuroscience and Medicine (INM-3), Research Centre Jülich, 52425, Jülich, Germany.
E-mail address: g.r.fink@fz-juelich.de (G.R. Fink).

http://dx.doi.org/10.1016/j.neuroimage.2017.07.054
Received 29 May 2017; Accepted 25 July 2017
Available online 26 July 2017

(2014) found increased movement-related β-ERD in ipsilateral primary motor cortex associated with higher age, implying a greater involvement of the ipsilateral hemisphere in older participants in order to maintain accurate motor performance (Boudrias et al., 2012; Ward et al., 2008; Zimerman et al., 2014). In stroke patients, ipsilateral α-ERD was found to be stronger than contralateral ERD when patients moved their paretic hand, which might again indicate a supportive role of ipsilateral motor cortex for recovered hand function (Steogonpień et al., 2011; Tangwiriyasakul et al., 2013; Verleger et al., 2003). Taken together, these findings are compatible with the idea that higher activity in ipsilateral motor cortex may contribute to maintaining motor performance across different contexts (Grefkes et al., 2008a; Zimerman et al., 2014). In contrast, much less is known about how iSM activity is influenced by the type of movement initiation.

As cortical motor areas operate in a network-like fashion, neural activity in iSM not only reflects local activity but also the influences that other areas exert upon iSM. One potential mechanism that could modulate iSM activity is inter-hemispheric 'cross-talk' with cSM (Hsieh et al., 2002; Kobayashi et al., 2003; B. van Wijk et al., 2012). Apart from contralateral SM, premotor areas (PM) known to be involved in many aspects of movement initiation could also exert an effect on iSM (Boenstrup et al., 2014; Cincotta et al., 2004; B. Van Wijk et al., 2012). Furthermore, such influences may depend upon whether the movement is stimulus-cued or self-initiated (Herwig et al., 2007; Krieghoff et al., 2011; Waszak et al., 2005). Stimulus-cued actions have been demonstrated to be preferentially mediated by a fronto-lateral network including the dorsal premotor cortex as well as the posterior parietal cortex (Obhi and Haggard, 2004; Toni et al., 2001; Waszak et al., 2005). In contrast, self-initiated actions have been shown to be predominantly mediated by a fronto-medial motor network in which the supplementary motor area (SMA) takes a prominent role (Desmurget and Sirigu, 2009; Eagleman, 2004; Jahanshahi et al., 1995; Mueller et al., 2007). Given the context-dependent roles of PM in the generation of self-initiated and stimulus cued movements, it is reasonable to assume that the oscillatory coupling between these regions and iSM also varies depending on how a movement is initiated.

Integrating these considerations about a context-dependency of iSM function and connectivity, we reasoned that the pre-movement ERD in the α- and β-frequency bands over iSM in a particular movement initiation context could be related to the context-dependent configuration of oscillatory coupling of iSM to the PMs and cSM. In order to test this possibility, we acquired EEG data (64-channel) while healthy participants generated button presses with their left or right index fingers either in a *Self-initiated* context or in a *Visually-cued* context.

To this end, we used phase coherence as a measure of connectivity as it has been widely interpreted as an indicator of functional coupling (Gerloff et al., 1998; Lachaux et al., 1999). Even though the focus of our study is on the ERD in iSM in the α- and β-bands, a role of premotor areas has been reported for several frequency bands. For example, when comparing internally and externally paced finger extensions, Gerloff and colleagues found that the internally paced movements exhibited a stronger coupling between the contralateral primary sensorimotor cortex and the medial premotor areas in a narrow β-band (20–22 Hz) (Gerloff et al., 1998). However, executive functions like cognitive control and monitoring of movements have been shown to be associated with changes in θ power (4–8 Hz) in the lateral and medial frontal cortex and phase synchronization between frontal electrodes in the θ band (Cavanagh and Frank, 2014; Cohen and Donner, 2013). Recently, we found that phase locking in the δ–θ frequency band (2–8 Hz) is a ubiquitous movement-related signal associated with movement execution across different movement initiation contexts (Popovych et al., 2016). To explore these alternatives, we considered the functional coupling of iSM to the premotor and other task-relevant motor regions across multiple frequency bands, namely, the δ–θ band, α-band, and the β-band.

We hypothesized that brain regions, which initiate iSM oscillatory activity, should exhibit a high phase coupling of their EEG rhythm with iSM during movement preparation, and, that such a coupling, if present, could occur in different frequency bands dependent upon the movement-initiation context (Gerloff et al., 1998). Furthermore, we hypothesized that such connectivity differences, if present, could be associated with the modulation of α- and β-ERD in iSM.

2. Materials and Methods

2.1. Participants

Twenty-one right-handed healthy participants (10 females, 11 males; age range: 22–35 years) participated in the experiment and were remunerated. All participants had normal vision, were right-handed (mean handedness score = 0.9) according to the Edinburgh Handedness Inventory (Oldfield, 1971), and had no prior history of psychiatric or neurological disease. Participants provided their written informed consent prior to the experiment. The study had been approved by the local ethics committee of the Faculty of Medicine, University of Cologne. Three of the 21 participants were excluded from data analysis due to data quality considerations, as described below.

2.2. Experiment design

2.2.1. Paradigm

The paradigm consisted of three conditions, namely, (i) the *Self-initiated* condition, (ii) the *Visually-cued* condition, and (iii) the *Vision-only* condition (see Fig. 1). The trials in each of the three conditions were organized into blocks of about 65 s duration. Each block started with an instruction (displayed for 2s) specifying the condition for the upcoming trials, following a 2–4s jitter time and 60s duration of task. On completion of a block, a feedback screen was displayed for 3s. The different blocks were marked by differential appearances of the fixation dot in order to remind the subject of the specific task that they had to perform (see Fig. 1). After the offset of the feedback on the screen, the fixation dot returned to its basic, unadorned form and the next task block followed after a baseline of 10s.

In the *Self-initiated* condition (Fig. 1A), participants were required to voluntarily produce a sequence of single index-finger button presses over the entire block. Apart from the fixation point that was displayed on the computer screen for the entire duration of the block, there were no additional stimuli to indicate (i) when and (ii) with which hand these button presses were to be produced. However, in order to prevent a response bias that would distort the EEG results, participants were instructed to approximately balance the number of left and right index finger button presses, while avoiding a systematic response pattern (e.g., Left-Right-Left-Right) and counting mentally the responses. In addition, participants were asked to produce button presses at intervals ranging from 4 to 8 s. After each block of the *Self-initiated* condition, participants were provided with performance feedback to help them better monitor and, if necessary, adjust their behavior. The extent of unbalanced button presses of one hand in a block was quantified as the absolute difference between the proportion of right index finger button presses and the proportion of left index finger button presses over the block, i.e., $100 \times |N_{right} - N_{left}|/(N_{right} + N_{left})$, where N_{right} and N_{left} are the number of right and left index finger button presses. Performances with unbalanced responses in the range 0%–30% received the feedback message "Well done". If the proportion of unbalanced responses was greater than 30% then the message "Unbalanced" was displayed as a warning. The 30% threshold was chosen so that the demand on the participant was neither too strict nor too lenient. Additionally, the participants received the feedback message "Well done" if they produced 8 to 12 button presses in one block, or a warning message if the number of button presses fell outside this range. A warning message "Too fast" was displayed if more than 12 button presses and the warning message "Too slow" when fewer than 8 button presses were produced in a block. Apart from these constraints, participants were free when and with which hand to generate

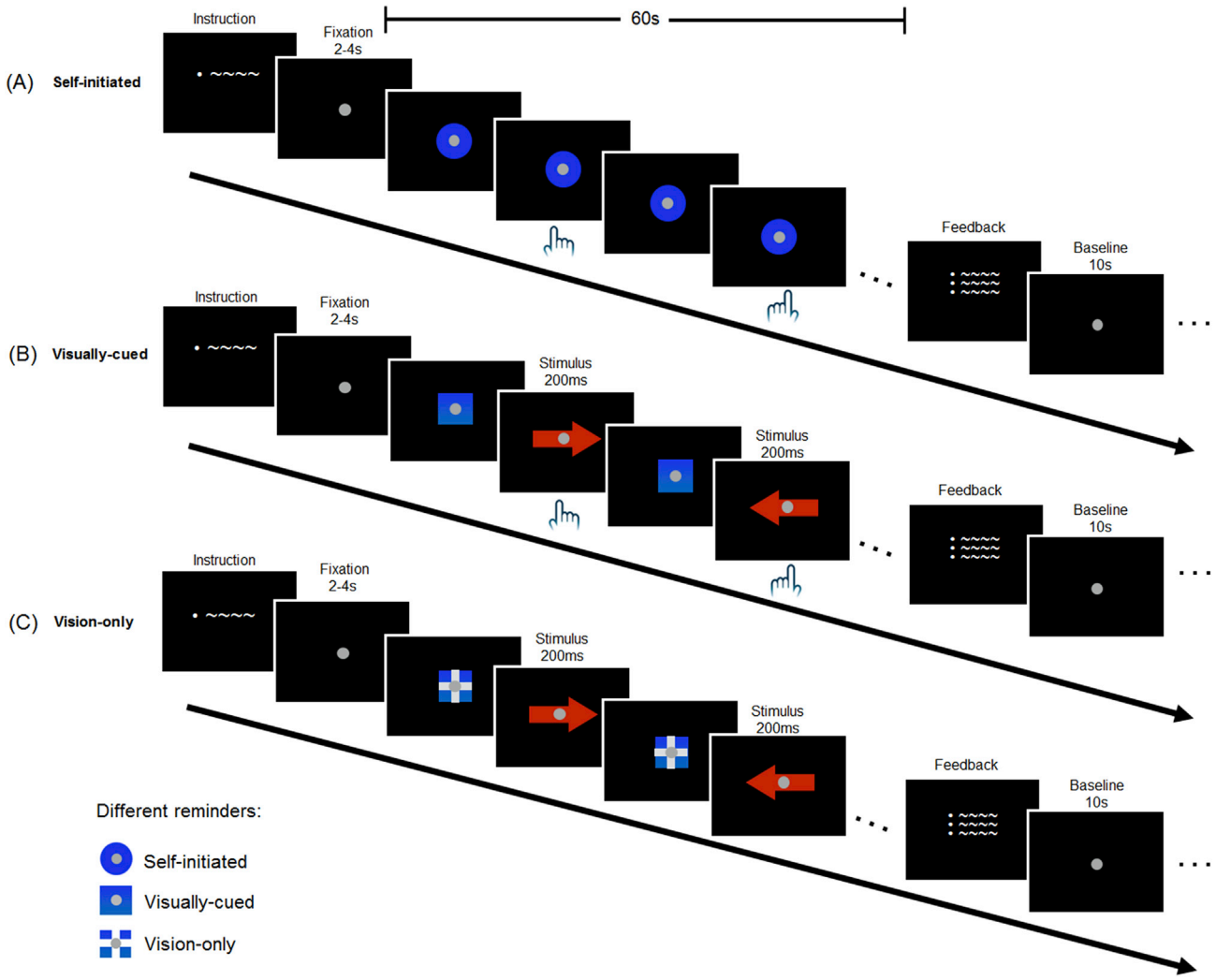

Fig. 1. The blocks representing the *Self-initiated* (A), the *Visually-cued* (B), and the *Vision-only* condition (C) in our study. The white fixation dot was displayed on the screen for 2–4s between the instruction and beginning of every block, which in total lasted 60s. The concentric blue disc, which was augmented by the white fixation dot, was used as an indicator of the *Self-initiated* condition. The hands represent the self-initiated button presses at a self-chosen time (A). The solid and broken blue square augmented by the fixation dot indicated the *Visually-cued* (B) and the *Vision-only* (C) conditions, respectively. The red arrow pointing to the left or right triggered the subject to press the button with their left or right index finger, respectively, in the *Visually-cued* condition (B). No button press was to be performed in the *Vision-only* condition (C). On completion of a block, a feedback was displayed on the screen. After the offset of the feedback on the screen, the fixation dot returned to its basic, unadorned form, and the next task block followed after a baseline period of 10s. Participants always performed the *Self-initiated* condition first (for details, see Methods), and the *Visually-cued* and *Vision-only* conditions followed in random order.

a movement.

In the *Visually-cued* condition (Fig. 1B), stimuli were displayed during the block that defined when and with which index finger the responses were to be produced. The stimulus in each trial was a red arrow (width: 2° visual angle, height: 1.2° visual angle) that pointed either to the right or to the left, and was displayed for 200 ms. Participants had to respond to this stimulus by pressing a button with the index finger corresponding to the arrow's direction. At the end of the block, the feedback screen displayed the message "Well done" when the accuracy was greater than 90% and a warning message if the response accuracy was below 90%.

A *Vision-only* condition (Fig. 1C) was employed for control. The condition was used to estimate EEG activity evoked by the visual stimuli in the absence of response-related activity. All stimulus materials and display parameters were identical to those employed in the *Visually-cued* condition. However, in the *Vision-only* condition, participants were instructed to attend only to the arrow stimuli without executing a corresponding motor response. Additionally, participants were instructed to refrain from motor imagery. At the end of the block, the feedback screen displayed the message "Well done" if no buttons had been pressed, and a warning message if erroneous button presses had occurred during the block.

The whole experiment lasted about 70 min and consisted of 16 blocks per condition. These 16 blocks were divided into 4 runs with each run (approximately 17 min long) containing four blocks of each condition. The blocks contained all three conditions, which were organized into triplets where the *Self-initiated* condition block was always presented first followed by the *Visually-cued* and *Vision-only* conditions (the order of these latter two blocks was randomized).

2.2.2. Inter-trial intervals

As the responses in the *Self-initiated* condition were voluntarily generated in the absence of external stimuli, (i) the total number of responses produced, (ii) the proportion of right and left hand responses, and (iii) the time interval between consecutive responses could vary in an idiosyncratic manner from block to block, which could limit the comparability of the different conditions (for example, producing large differences in the number of trials per condition). To address these concerns, we matched the trial structure across conditions: the number of trials and inter-stimulus intervals (ISI) in the *Visually-cued* and *Vision-only* conditions were adaptively defined based on the participant's behavior in

the *Self-initiated* condition (Michely et al., 2015, 2012). This adaptive procedure ensured that the total number of responses, the proportion of left/right responses, and the timing between responses were closely matched across conditions. If the response intervals in the *Self-initiated* condition were shorter than 4s, these short intervals were replaced online with randomly chosen intervals in the range of 4–8s. This adaptive procedure limited the influence of poorly timed responses in the *Self-initiated* condition on the other conditions. After the experiment, we analyzed the behavioral data to assess that the participants had followed the experimental instructions. Consistent with these instructions, the mean inter-response interval (IRI) was 6618 ms ± 136 ms standard error (SE). Furthermore, the proportion of right and left responses was well balanced (50.7% right index finger, 49.3% left index finger). In the *Self-initiated* condition, only 1.8% of the inter-response intervals were shorter than 4s. Trials with such short intervals were removed from the *Self-initiated* condition prior to further analyses. In the Visually-cued condition, the mean accuracy is 97.7 ± 0.5%.

2.2.3. Training procedure

Participants were familiarized with the experimental procedures before the start of the actual experiment, and underwent instruction and training while the EEG-cap was applied. Participants first practiced the *Visually-cued* condition. The arrows were presented every 4–8 s (i.e., the desired timing for the *Self-initiated* condition). When participants were familiar with this condition, training of the *Self-initiated* condition followed. Participants were instructed to freely choose the time to respond and the finger to move, with the guideline to produce responses at approximately the same frequency as the stimulus frequency in the *Visually-cued* condition that they had just practiced. Additionally, participants were instructed to approximately balance the number of left and right index finger button presses, while avoiding a systematic response pattern (e.g., Left-Right-Left-Right) and mental counting of the responses or the time-intervals. Training lasted until participants showed a stable response rate and a clear understanding of the instructions. During the experiment, if participants received warnings related to either balance or timing on two successive blocks of the *Self-initiated* condition, the experiment was interrupted and participants were re-trained until they could meet the task demands of the *Self-initiated* condition before resuming the session.

2.3. Apparatus

Scalp EEG was recorded using a 64-channel active electrode system (actiCAP, Brain Products GmbH, Munich, Germany) mounted to the head according to the extended 10–20 international system in a spherical array.

All stimuli were generated and displayed using the software "Presentation" (version 11.0, Neurobehavioral Systems, Berkeley, CA) on a 47 cm × 29 cm LCD monitor with a screen resolution of 1280 × 1024 pixels, and a refresh rate of 60 Hz. Index-finger responses were collected in two different ways. Button-presses were registered by two LumiTouch key-pads (Photon Control Inc., Burnaby, BC, Canada), one for each hand. Movements of the index finger of each hand were measured with an acceleration sensor (Brain Products GmbH, Munich, Germany) attached to the dorsal-tip of the index finger. Each sensor was 22 mm × 14 mm x 8 mm in size; weighed 8 g and had a sensitivity of 420 mV/g. The sensors provided output voltages that were directly integrated into the EEG recording as additional channels. Each sensor provided three voltage signals corresponding to instantaneous acceleration of each finger along three orthogonal axes (*X, Y, Z*) in a Cartesian coordinate system centered at the fingertip. We used accelerometers as our key measure of motor-output as the acceleration signals are highly sensitive and are not restricted to a muscle group and a specific movement direction like surface EMG (Keil et al., 1999). Additionally, the use of accelerometers allowed us to exclude trials with unnecessary movements or mirror movements.

2.4. EEG data acquisition and processing

2.4.1. EEG data acquisition

After EEG capping, participants were seated in a comfortable chair with their head supported by a chin-rest in a sound proof room. Accelerometers were firmly attached to the dorsal tip of both index fingers with an adhesive tape. Participants were instructed to minimize eye-blinks and to maintain fixation at all times during the task blocks. Additionally, they were asked to minimize unnecessary movements of the body and the index fingers.

From the 64 electrodes, three electrodes (FT9, FT10 and TP10 in the 10–20 system) were removed from their position on the scalp and placed at the bilateral outer canthi and under the left eye to record bilateral horizontal and left vertical electro-oculograms (EOG). All electrodes were originally referenced online to the left mastoid. At the beginning and end of the recording, the impedance of the electrodes was assessed to ensure that impedances of all electrodes were $\leq$15 kΩ. EEG signals were amplified, band-pass filtered from 0.1 to 250 Hz, and digitized at a sampling rate of 2500 Hz.

2.4.2. EEG data preprocessing

The preprocessing and analysis of the EEG data were implemented using the EEGLAB toolbox (Delorme and Makeig, 2004) and in-house scripts developed in Matlab R2015b (MathWorks Inc.)

The raw data were first bandpass filtered from 0.5 to 48 Hz to increase the signal-to-noise ratio and to avoid a potential of 50 Hz as an electric current artifact and then downsampled from 2500 Hz to 200 Hz. Next, the continuous raw EEG data were visually inspected for paroxysmal and muscular artifacts not related to eye blinks. Noisy portions of the signal were excluded from further analysis. All trials in the *Visually-cued* condition with incorrect responses were excluded, as well as trials with response times (RT) greater than 1s. In the *Self-initiated* condition, button presses preceded by an inter-response interval of less than 4s were excluded. Additionally, in all conditions the accelerometer recordings were used to exclude trials with unnecessary finger movements prior to the movement onset, as well as any trials with mirror movements.

The movement onset was defined based on the accelerometer recordings as follows: the first derivatives of the X, Y, and Z components of the acceleration signal were computed and then combined to obtain the scalar (Euclidean) magnitude of the instantaneous acceleration change at each time point. This time-series was then smoothed, rescaled, and a threshold was set to identify the earliest time point in a 125 ms window prior to each button press that showed a continuous increase in acceleration rate. All trials where the movement onset could not be unambiguously detected were excluded from further analyses.

The continuous EEG data were then segmented for the three conditions. Epochs in the *Self-initiated* condition were defined from −2.5s to 1.5s relative to movement onset. The epochs for the *Visually-cued* condition, were defined from −2.0s to 1.5s relative to movement onset. The context-specific differences of the *Self-initiated* and *Visually-cued* conditions prompted us to define the baseline period differently in the two conditions leading to epochs of differing duration relative to movement onset. In a self-initiated motor task, the preparatory brain activity related to selection could begin at an undefined period, even as early as 2s before movement onset (Haggard, 2008). To limit confounds due to this preparatory activity we used a baseline as early as possible in the *Self-initiated* condition (from −2500 to −1500 ms). However, the epoch for the *Visually-cued* condition could not be exactly matched with the one of the *Self-initiated* condition even though the *Visually-cued* condition was based on the inter-response intervals obtained in the *Self-initiated* condition. The reason for the latter is the variable reaction time in the *Visually-cued* condition. Therefore, the minimum interval between two button-presses in the *Visually-cued* condition could be shorter than the defined inter-stimulus intervals of 4s. Accordingly, we selected a baseline (from −2000 to −1000 ms) that fell in all trials prior to stimulus onset because all trials with RT > 1000 ms were discarded, and eliminated any

overlap in the epochs of consecutive trials. Of note, the activities in the *Visually-cued* and *Vision-only* condition were quite similar before the onset of the stimuli, therefore we segmented the *Visually-cued* and *Vision-only* conditions into 4s epochs from −1.5s to 2.5s relative to the onset of stimuli, and the time period −1500 to −500 ms was used as the baseline.

After segmenting the continuous EEG data, the obtained epochs were corrected for artifacts. First, epochs were rejected if the amplitude over the entire epoch was larger than 100 μV or showed an abnormal drift that exceeded 75 μV. Next, a semi-automated procedure based on independent component analysis (ICA) was used to identify epochs contaminated by artifacts such as blinks, eye movements, muscle activity, and infrequent single-channel noise. The independent component decomposition was performed using the Infomax ICA algorithm implemented in EEGLAB. The ADJUST algorithm (Mognon et al., 2011) was then used to identify and reject components containing blink/oculomotor or other artifacts that were distinguishable from the rest of the brain activity. Noisy channels were detected automatically by EEGLAB and interpolated using spherical spline interpolation. Finally, the artifact-free trials were average-referenced and baseline-corrected.

The data of three participants had to be excluded from further analyses as there was an insufficient number of trials that satisfied all the quality criteria described above. The data of one participant had a large number of artifact-contaminated epochs because of eye-movements; and two participants showed a large number of task-irrelevant movements during the baseline period as detected by the accelerometer. Thus, data from 18 participants were included in the further analyses. After removing trials that contained an artifact, or that had an IRI less than 4s in the *Self-initiated* condition, or a RT of more than 1s in the *Visually-cued* condition, a minimum of total 100 artifact-free trials (100–160 for *Self-initiated*, 104–161 for *Visually-cued* condition) were obtained for each subject. All further analyses are solely based on these trials.

2.4.3. Spatial filtering

A crucial part of our data processing, which we performed before the time-frequency transformation and the coherence analysis, was the spatial filtering. We used the Laplacian transformation as it reduces volume conduction from distal sites, thereby enhancing spatial resolution and enabling analyses of electrodes close to the region of interest (Tenke et al., 2012). Surface Laplacians were estimated from the individual artifact-free EEG epochs using a spherical spline algorithm (Perrin et al., 1989) provided by the current source density (CSD) toolbox implemented in Matlab (Kayser and Tenke, 2006). CSD waveforms were computed for each original surface EEG potential (50 iterations, degree of spline = 4). As the surface Laplacian can attenuate low spatial frequencies that can be attributed to volume conduction, it is therefore appropriate for the use of connectivity analyses (Cohen, 2014). Though not a source localization analysis, Laplacian renders the electrodes maximally sensitive to radial sources directly underlying each electrode (Tenke et al., 2012). This means that after the Laplacian transform, the neurophysiological signals collected from electrodes situated above certain brain areas in specific time windows can be regarded as indices of the activation of the underlying brain structure (Rigoni et al., 2013; Steinmetz et al., 1989).

2.4.4. Estimation of spectral power

The spectral power is revealed by the *event-related spectral perturbation* (ERSP) that was computed from the Laplacian-transformed EEG data. The ERSP measures average dynamic changes in the EEG amplitude spectrum induced by a set of experimental events in the broad band frequency as a function of time. We calculated the ERSP to test our hypothesis that the pre-movement ERD in the α and β band is differentially modulated by how a movement is initiated (Meirovitch et al., 2015; Notturno et al., 2014; Pfurtscheller, 1989, 1981; Pfurtscheller et al., 2006). The calculation of the full-spectrum ERSP yields more information on brain dynamics than calculation of only the narrow-band ERD, because spectral changes typically involve more than one frequency or frequency band (Makeig, 1993). To compute the ERSPs, the Laplacian-transformed EEG signals of each channel were decomposed into the time-frequency domain using complex Morlet wavelets with the number of cycles linearly increasing from 3 to 9 as the frequency increases. The purpose of doing this was to adjust the ratio of time/-frequency resolution along the frequency axis, and to get the best trade-off between time and frequency resolution (Makeig, 1993). Then, the ERSP in each frequency was normalized by subtracting the baseline spectrum value averaged over the baseline period for each frequency. The baseline excluded the period that contained edge artifacts resulting from applying temporal filters in the Morlet wavelets convolution. Considering the distinct topographies and functions of the different movement-related frequency bands, we investigated the spectral power in the α (8–13 Hz), low-β (13–21 Hz), high-β (21–30 Hz), and γ (30–48 Hz) band, separately.

The processing and analysis steps described above were implemented using the EEGLAB toolbox (Delorme and Makeig, 2004) and custom scripts in MATLAB (MathWorks, USA).

2.4.5. Estimation of phase-based coherence

The phase-based coherence over trials between pairs of electrodes was computed from the Laplacian-transformed EEG data as a measure of functional connectivity over the whole frequency band (2–48 Hz). The advantage of coherence over trials is that it provides not only stronger evidence for task-related modulation in connectivity, but also more temporal precision as it is computed at each time point in the time interval of interest (Cohen, 2014). Coherence has been widely used as a normalized measure of temporal synchronization between pairs of EEG channels in a given frequency band (Babiloni et al., 2006; Storti et al., 2015). The coherence $Coh_{x,y}(t,f)$ between two given electrodes x and y at time t in the frequency band f is calculated by:

$$Coh_{x,y}(t,f) = \left| N^{-1} \sum_{n=1}^{N} e^{i\left(\varphi_{n,x}(t,f) - \varphi_{n,y}(t,f)\right)} \right|$$

in which N refers to the total number of trials, and $\varphi_{n,x}$ and $\varphi_{n,y}$ are the phase angles from electrodes x and y on trial n. Here, an increase in EEG coherence (scale from 0 to 1) can be interpreted as an enhancement of functional connectivity and information transfer (i.e., functional coupling or binding). This measure is also often referred to as phase-locking value (Lachaux et al., 1999).

In order to reduce the effect of inter-subject and inter-trial variation in these 'raw' coherence values, the relative coherence was calculated by subtracting the frequency band-specific baseline averaged over the whole baseline period from the raw coherence values. The baseline period was identical to that used for the preprocessing and power analysis. Finally, the obtained coherences in the δ-θ (2–8 Hz), α (8–13 Hz), low-β (13–21 Hz), and high-β (21–30 Hz) band were averaged for further analysis in order to find significant movement-related modulations of frequency-band-specific coherences based on previous studies (Cavanagh and Frank, 2014; Cohen and Donner, 2013; Popovych et al., 2016). This coherence analysis can only characterize the coupling between two distinct regions within one frequency band, and does not inform about the directionality and the quality of information flow, i.e., being it inhibitory or excitatory.

Importantly, both the spectral power and coherence in each frequency band were computed from averaged pairs of electrodes above the brain regions of interest in order to increase the signal to noise ratio (Rigoni et al., 2013; Steinmetz et al., 1989). According to the 10–20 system, the EEG signals from the C1 and C3 electrodes, which are located above the motor cortex of the left hemisphere, and the ones from C2 and C4, located over the motor cortex of the right hemisphere, were averaged, reflecting the activity of the ipsilateral sensorimotor cortex (iSM) for left and right hand movements, respectively. We used the iSM as seed

region and calculated its coherence with all other electrodes. The regions of interest were as follows: the median electrodes FCz and Cz were used to reflect the activity of the SMA, the lateral electrodes FC1 and FC3 (or FC2 and FC4) were used to reflect the activity of the contralateral (or ipsilateral) premotor areas (cPM/iPM). Although hand dominance may modulate the results, the hand effect was not in the focus of our current study. As we assume that the power changes for left- and right-hand movements were symmetrical, left- and right-hand movement trials were combined by considering the sensorimotor cortices as ipsilateral and contralateral sides to the hand movement to gain maximal sensitivity.

2.5. Linking spectral power over iSM to network-based phase-coherence

Prior studies have reported that in self-initiated unilateral actions the ERD is initially greater over the contralateral sensorimotor cortex, but becomes bilateral starting from around −500 ms (Bai et al., 2005; Pfurtscheller and Lopes Da Silva, 1999). The corresponding ERD dynamics for stimulus-cued actions are not well characterized. To avoid circular inferences in choosing a data-driven time period (Cohen, 2014), here, we focused our analysis on a 500 ms period immediately preceding movement onset (i.e., from −500ms to 0 ms) to evaluate the possibility that pre-movement ERD in the α- and β-frequency bands over iSM in a particular movement initiation context could be related to the context-dependent configuration of oscillatory coupling of iSM to the premotor regions and cSM. The mean power and mean phase coherence over this period were the basis for our analysis. To link ERD to coherence, we used a Spearman correlation between the mean phase-coherence and the mean spectral power in SM over the pre-movement period in each frequency band. This nonparametric correlation method was used because both power and coherence data are non-normally distributed and may contain outliers.

3. Results

3.1. Lateralization of ERD is modulated by movement-initiation context

Prior to the movement onset, the oscillatory power in the α, low-β, and high-β frequency bands over the contralateral and ipsilateral SM revealed a context-specific modulation (Fig. 2). In the *Self-initiated* condition, the decreases in power were found not only over cSM, but also over iSM, starting around 500 ms prior to movement onset (Fig. 2A). In the *Visually-cued* condition, bilateral decreases in power were also pronounced in the α, low-β, and high-β frequency bands but with the largest changes occurring in the period immediately prior to movement onset (Fig. 2B).

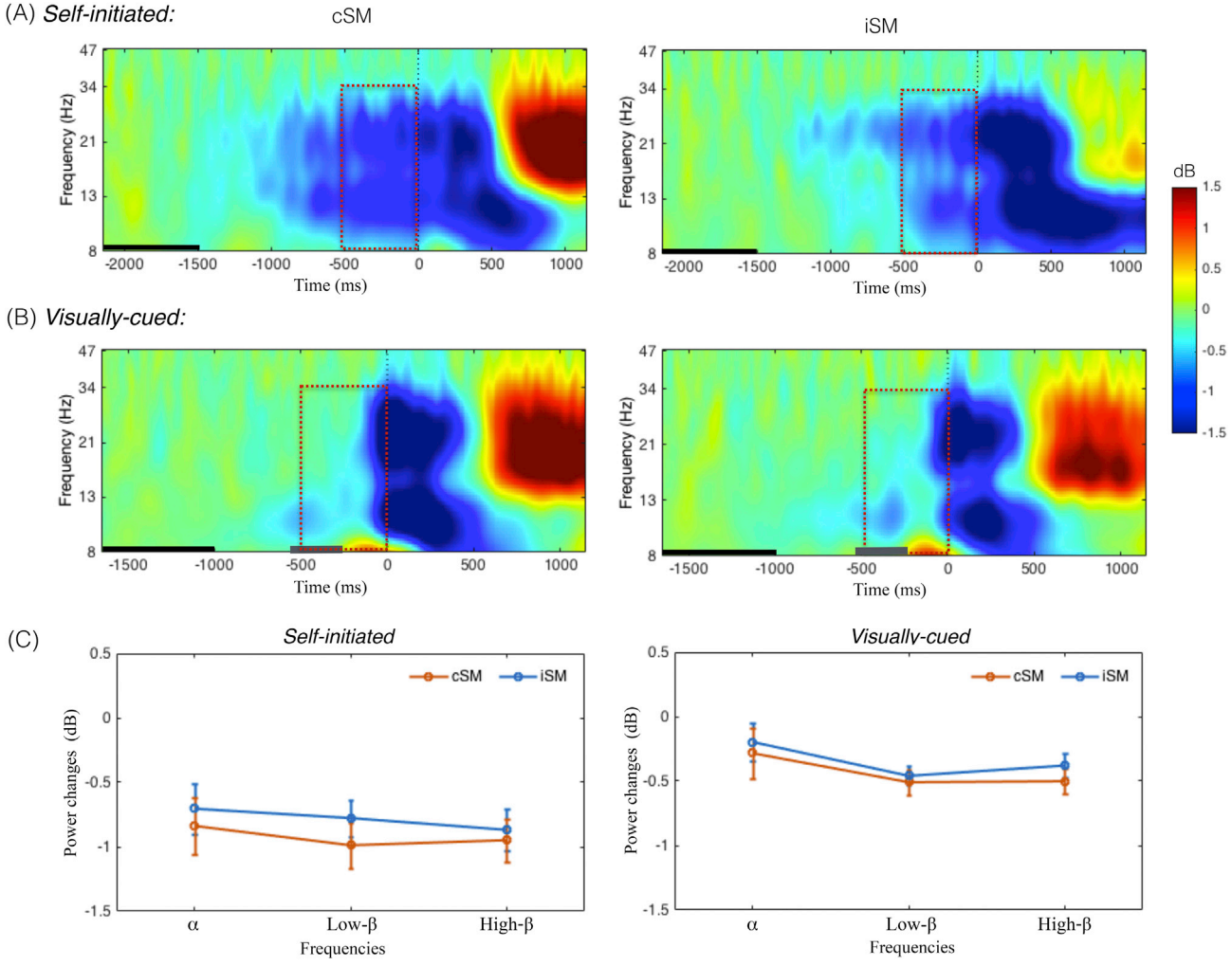

Fig. 2. Time-frequency spectra over contralateral (cSM) and ipsilateral sensorimotor cortex (iSM) time-locked to movement onset in the *Self-initiated* (A) and *Visually-cued* condition (B), respectively. The EEG signals from the C1, C3 electrodes over the left hemisphere and C2, C4 electrodes over the right hemisphere were averaged, reflecting the activity of the left SM and right SM, respectively. The left- and right-hand movement trials were combined by considering the sensorimotor cortices as iSM and cSM to the hand movement. The dashed boxes indicate the time and frequency of interest that were averaged for the ANOVA (C). The black horizontal lines represent the baseline period in both conditions, and the grey lines in (B) represent the period in which the visual stimuli were presented. (C) shows the result of the 3-way ANOVA analysis (conditions x frequencies x sides).

To assess the frequency-specific modulation of spectral power over cSM and iSM by the movement-initiation context, we submitted the mean frequency-specific power of SM over the time period −500 to 0 ms to a 3-factorial repeated-measures ANOVA with factors Condition {*Self-initiated, Visually-cued*}, Frequency {α, low-β, high-β}, and Side {contralateral, ipsilateral}. The 3-way interaction between these factors was not significant ($F(1,17) = 0.52$, $p = 0.60$). Only the 2-way interaction between condition and side was significant ($F(1,17) = 5.014$, $p = 0.038$), with a main effect of condition and side (condition: $F(1,17) = 17.96$, $p = 0.0006$; side: $F(1,17) = 19.54$, $p = 0.0004$; Fig. 2C). A post-hoc *t*-test to confirm the relationship between condition and side revealed that the power over cSM exhibited a significantly greater decrease than the power over the iSM in the *Visually-cued* condition ($t(17) = 2.19$, $p = 0.028$), but not in the *Self-initiated* condition ($t(17) = 1.81$, $p = 0.09$). These results indicate that the ERD prior to movement onset showed a greater contralateral preponderance in the *Visually-cued* context but not in the *Self-initiated* context, where the ERD was more bilaterally distributed. Furthermore, the difference of spectral power within three frequency bands was not modulated by the movement initiation context.

To investigate the effect of stimulus-related power changes over the posterior electrodes on movement production, we analyzed the power changes over the sensorimotor cortex in the *Visually-cued* and the *Vision-only* conditions time-locked to the onset of the visual stimulus (i.e., $t = 0$ is the onset of the visual stimulus, see supplementary materials and Fig. S1). These results confirmed that the pre-movement power changes in the *Visually-cued* condition over the sensorimotor regions in the α- and β-band were indeed related to movement production and not evoked by visual stimulus processing due to volume conduction effect.

Topographical maps showed that the power decreases in the α and β frequency bands were localized in the sensorimotor cortex for both conditions (Fig. 3). In addition, power changes were also observed in areas over the midline (i.e., the SMA region) in the *Self-initiated* condition, and over parietal and occipital cortex in the *Visually-cued* condition (Fig. 3). In addition, we also plotted the time-frequency spectra for the other regions of interest in the two conditions (i.e., SMA, iPM and cPM) in the supplementary materials (Fig. S2 and Fig. S3). We found that the pattern of ERD oscillations in α and β bands from these regions had a systematic difference, which suggests that Laplacian transformation can improve the activity localization and minimize the volume conduction effect.

In summary, we found that the lateralization of ERD in the sensorimotor cortex is modulated by different movement-initiation contexts.

3.2. Coherence in different frequency bands in different movement-initiation contexts

We next investigated the temporal synchronization between pairs of EEG channels in a given frequency band by using phase coherence.

The group-averaged phase-coherence of oscillations in iSM to all other electrodes over the scalp showed a strong qualitative difference between contexts, with a prominent role of the δ-θ-band in the *Visually-cued* context but not in the *Self-initiated* context for both hands (Fig. 4A). However, the group-averaged phase-coherence was more similar between the two initiation contexts in the α-band between iSM and other motor-related areas (Fig. 4B). In the subsequent analyses, left- and right-hand movement trials were collapsed by considering the sensorimotor cortices as ipsilateral and contralateral sides to the hand movement to gain maximal sensitivity.

To evaluate the frequency-dependent effects in the functional coupling of the iSM to other motor regions more closely (represented by their respective closest EEG electrodes, see Materials and Methods), we averaged the coherence over the period −500 to 0 ms for each coupling. Oscillations in iSM in the *Self-initiated* condition showed a significant mean phase-coherence to cSM and to SMA in the α-frequency band, but not to iPM or cPM (Fig. 5A, $t(17) = 4.30$ for cSM-iSM; $t(17) = 4.20$ for SMA-iSM, $p < 0.05/8$, Bonferroni corrected). The iSM exhibited no other

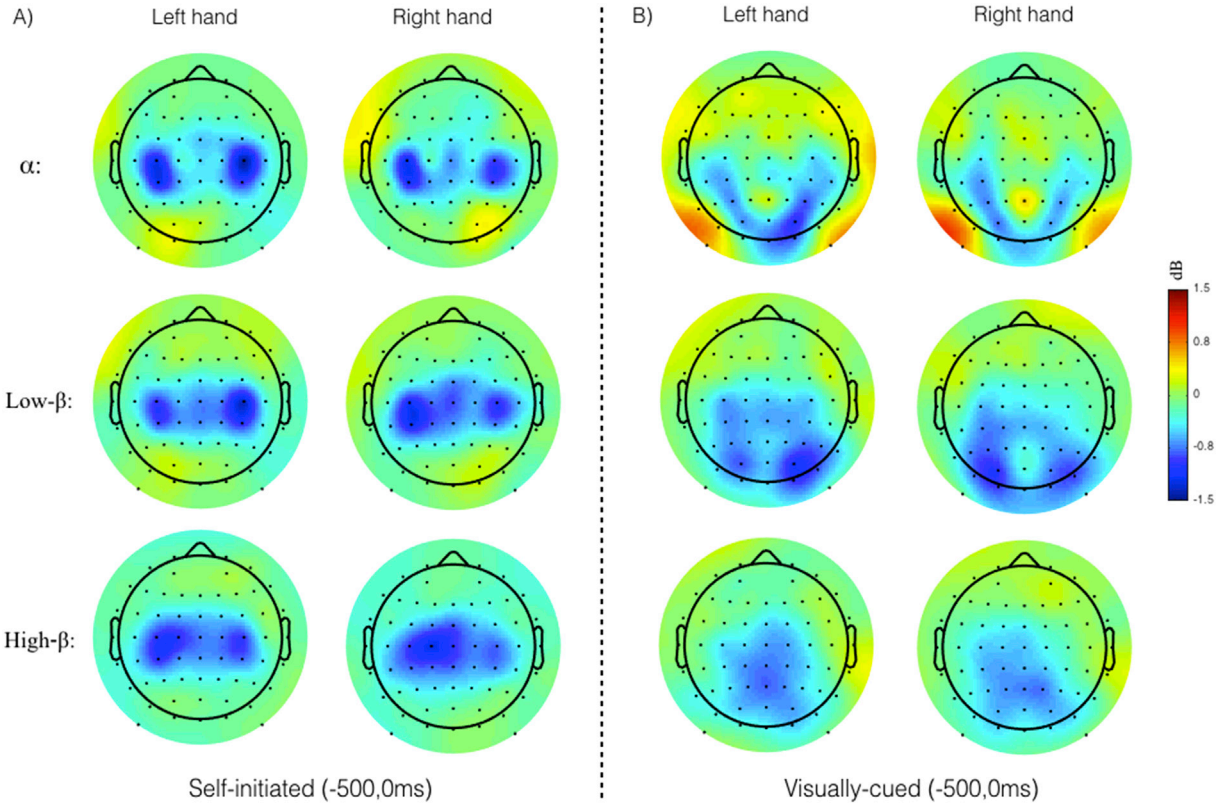

Fig. 3. The topographic map of averaged spectral power in a time period prior to movement onset, i.e. [-500,0] ms in the (A) *Self-initiated* and (B) *Visually-cued* condition in three typical ERD frequency bands. The frequency bands were defined as α (8–13 Hz), low-β (13–21 Hz), high-β (21–30 Hz).

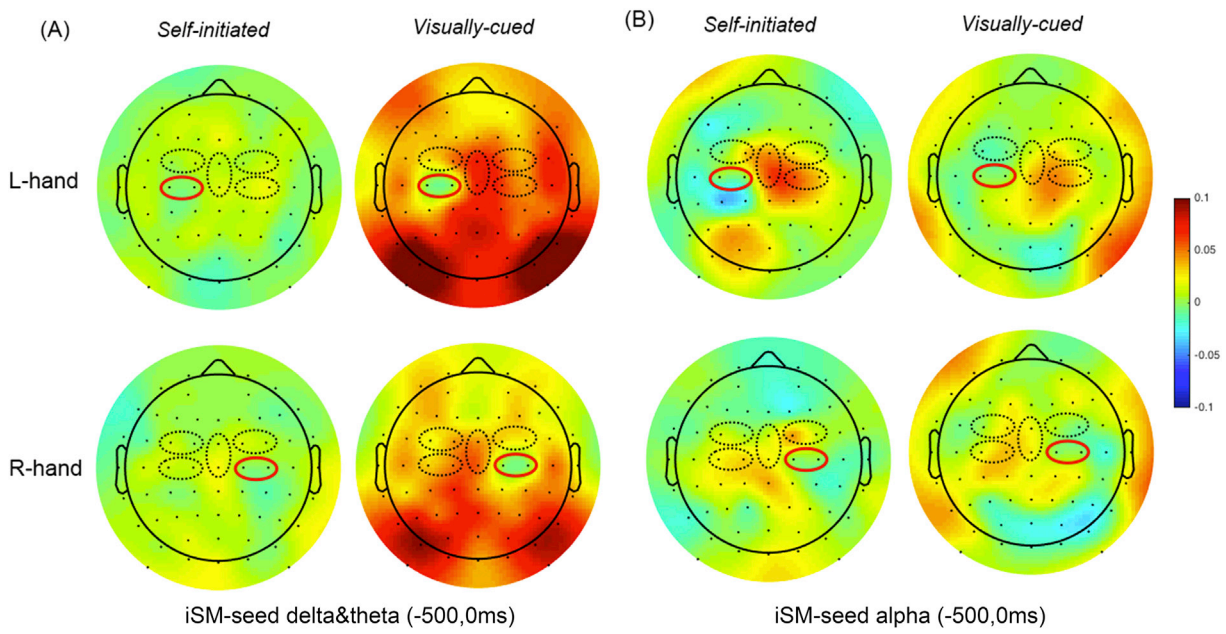

Fig. 4. Topographical maps of iSM-seeded coherence averaged in the interval [-500,0] ms in the δ-θ (A) and α frequency band (B) for both conditions. The results are shown for the left and right hand, separately. The red ellipses represent the seed regions; black dashed ellipses represent regions of interest in the motor system. In the seed-based coherence analysis, we did not calculate the self-connected coherence of the seed regions. Therefore, the self-connected coherence value (in the red ellipse) is '0'.

statistically significant coherence to any of these regions in the other frequency bands (i.e., δ-θ-band, or the low- and high-β, see supplementary table for detailed statistics). However, over the same time period, in the *Visually-cued* condition, the α-band oscillations in iSM were only coherent to cSM but not to SMA or either PM areas (Fig. 5B, $t(17) = 3.90$, $p < 0.05/8$, Bonferroni corrected). With the exception of cPM-iSM, the mean coherence of iSM with all the other regions were statistically significant in the δ-θ-band (Fig. 5B, $t(17) = 3.40$ for cSM-iSM, $t(17) = 4.60$ for SMA-iSM, $t(17) = 4.90$ for iPM-iSM; $p < 0.05/8$, Bonferroni corrected, please see the supplementary table for detailed statistics).

We next assessed the modulation of coherence magnitude during the time period [-500,0] ms by the movement-initiation context in the frequency bands of interest, i.e., the ones that exhibited significantly

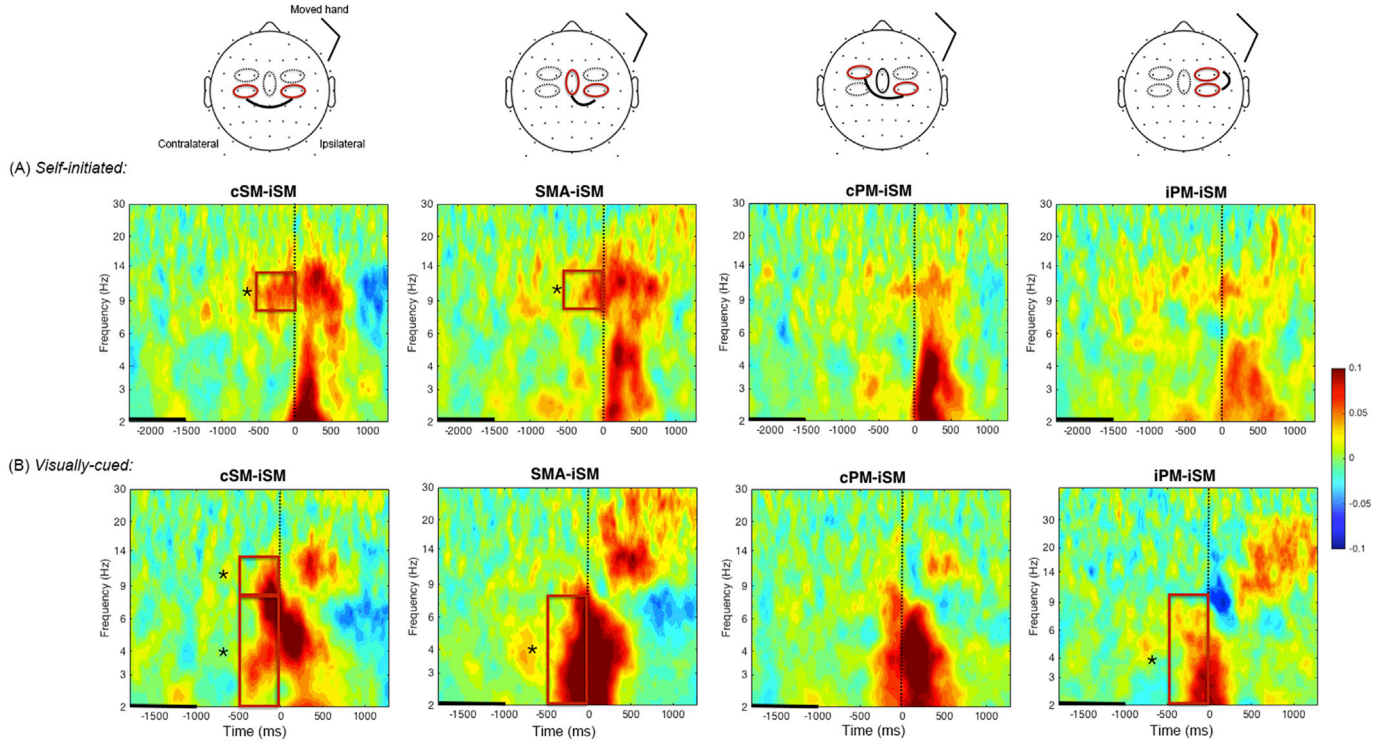

Fig. 5. Phase coherences of cSM-iSM, SMA-SM, cPM-iSM, and iPM-iSM in the *Self-initiated* (A) and *Visually-cued* condition (B). The phase coherence of left- and right-hand movement trials were combined as ipsilateral and contralateral sides to the hand movement to gain maximal sensitivity. The red rectangles indicate the significantly increased coherence in corresponding frequency bands during the period [-500, 0] ms relative to the baseline. The black lines represent the baseline period. The cartoon brains above represent the couplings that are shown by the plots below.

different coherences compared to baseline in α- and δ-θ-bands. We evaluated whether the mean phase-coherence between iSM and cSM was modulated by movement-initiation context with a 2-factor repeated-measures ANOVA with factors Condition {*Self-initiated*, *Visually-cued*} x frequency {δ-θ, α}. The interaction of these factors was significant [Condition x frequency: F (1,17) = 6.27, p = 0.02; Condition: F (1,17) = 0.54, p = 0.47; Frequency: F (1,17) = 3.06, p = 0.10]. A post-hoc *t*-test showed that the coherence between iSM and cSM in the δ-θ band was greater in the *Visually-cued* condition than in the *Self-initiated* condition (Fig. 6A, t (17) = 2.15, p = 0.04). Importantly, the conditions did not differ statistically in α-band coherence (Fig. 6A, t (17) = −0.62, p = 0.55).

We also evaluated the coherence of SM-SMA with a 3-way ANOVA with factors Side {cSM-SMA, iSM-SMA} x Condition {*Self-initiated*, *Visually-cued*} x frequency {δ-θ, α} (Fig. 6B). The 3-way interaction was not significant (F (1,17) = 0.75, p = 0.40), but, importantly, the 2-way interaction of side and condition was significant (F (1,17) = 5.08, p = 0.03). The post-hoc *t*-test showed that contralateral preponderance of coherence was mainly observed in *Self-initiated* movements (t (17) = 2.28, p = 0.036), whereas coherence in *Visually-cued* movements was similar between contralateral and ipsilateral sides (t (17) = 0.93, p = 0.37). This modulatory role of condition on the coherence relationship between cSM-SMA and iSM-SMA shows that the SM-SMA coherence cannot, at least entirely, be ascribed to a common source due to proximity of electrodes.

3.3. Power changes over ipsilateral SM has a context- and frequency-specific relation to coherence-based connectivity

We next tested the link between oscillatory power at iSM and its connectivity by evaluating their correlation. For each inter-regional coupling to iSM that showed a statistically significant phase-coherence (section 3.2), we tested whether that coupling's mean phase-coherence was correlated with the power changes over iSM in each of the three frequency bands (α, low-β, and high-β). In the *Self-initiated* condition, the mean coherence of cSM-iSM in the α-band significantly correlated with ERD in iSM in the high-β frequency band (Fig. 7, $r = -0.79$, $p < 0.05/6$, Bonferroni corrected) but not in the α- and low-β bands. Furthermore, this was a negative correlation ($r = -0.79$), that is, a larger mean α-band coherence in the oscillations of cSM and iSM was associated with a larger decrease in high-β power relative to baseline over iSM. The mean α-band coherence of cSM-iSM was similarly correlated with the ERD over cSM ($r = -0.76$, $p < 0.05/6$, Bonferroni corrected). The corresponding correlations in the *Visually-cued* condition exhibited a different relation to ERD over iSM and cSM. The mean α-band coherence of cSM-iSM was correlated with ERD in iSM in the α-band (Fig. 7, upper panel, $r = 0.72$, $p < 0.05/6$, Bonferroni corrected) but not in the low- or high-β bands. Remarkably, this was a positive correlation ($r = +0.72$), with a larger mean α-band coherence of cSM-iSM being associated with a smaller decrease in α-band power over iSM. Furthermore, the α-band coherence of cSM-iSM was not correlated with ERD over cSM in any frequency band ($p > 0.05/6$, Bonferroni corrected). This difference between conditions is especially notable since the mean α-band coherence of this cSM-iSM coupling was not statistically different between conditions (Fig. 6A, section 3.2), and the mean power over iSM was not different between α-band and high-β bands in both conditions (Fig. 2C, section 3.1).

The correlation between the phase-coherence in SMA-iSM to the power changes over iSM showed a similar difference between conditions. In the *Self-initiated* condition, the mean α-band coherence of SMA-iSM (Fig. 7, lower panel) was negatively correlated with power over bilateral SM only in the high-β frequency band ($r = -0.60$ for iSM, $r = -0.61$ for cSM, $p < 0.05/3$, Bonferroni corrected). In the *Visually-cued* condition,

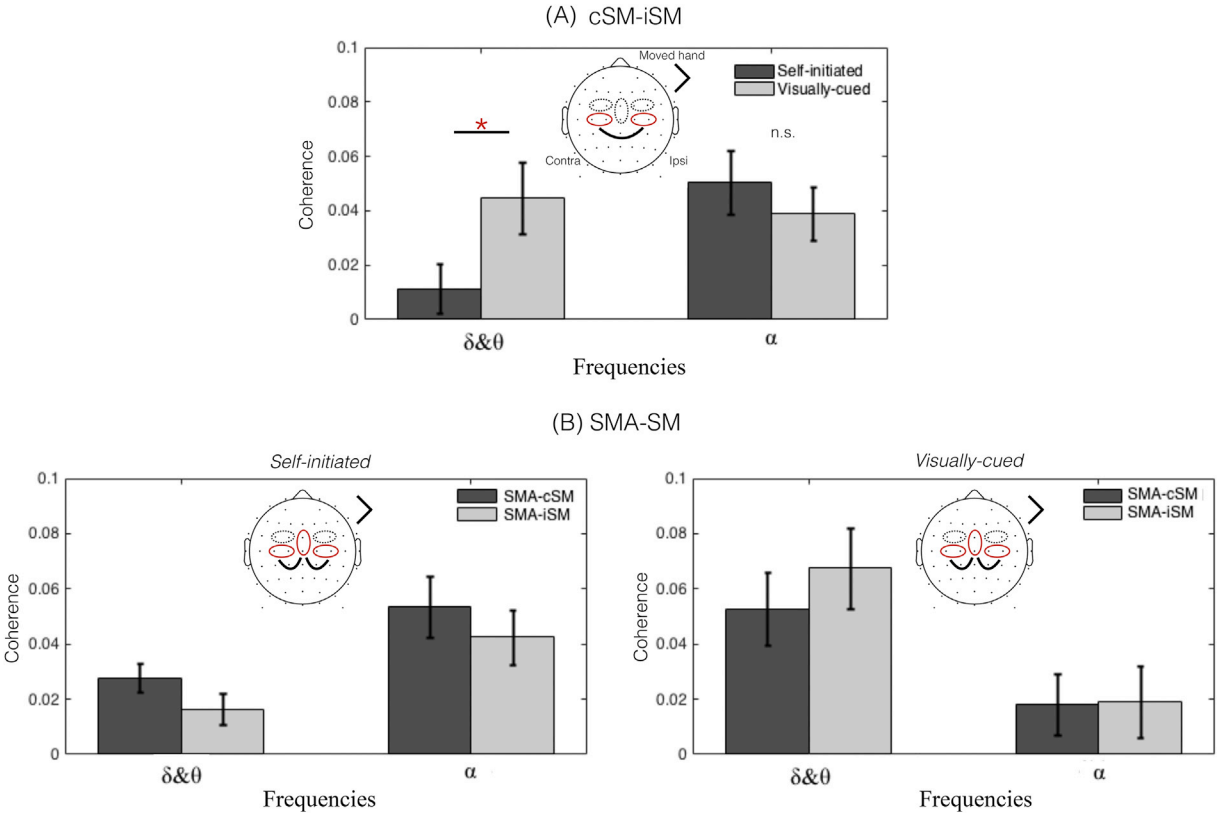

Fig. 6. The ANOVA comparison of the coherences for cSM-iSM (A), and SMA-iSM (B). The mean phase-coherence between iSM and cSM was submitted to a 2-factor repeated-measures ANOVA with factors Condition {*Self-initiated*, *Visually-cued*} x frequency {δ-θ, α}. The mean phase-coherence between iSM and SMA was submitted to a 3-factor repeated-measures ANOVA with factors Condition {*Self-initiated*, *Visually-cued*} x frequency {δ-θ, α} x side {SMA-iSM, SMA-cSM}. The error bars represent the standard error of the mean (SEM). The red star indicates the significant difference in coherences ($p < 0.05$) revealed by post-hoc analysis. The cartoon brains in the figures represent the couplings that were tested by the ANOVA.

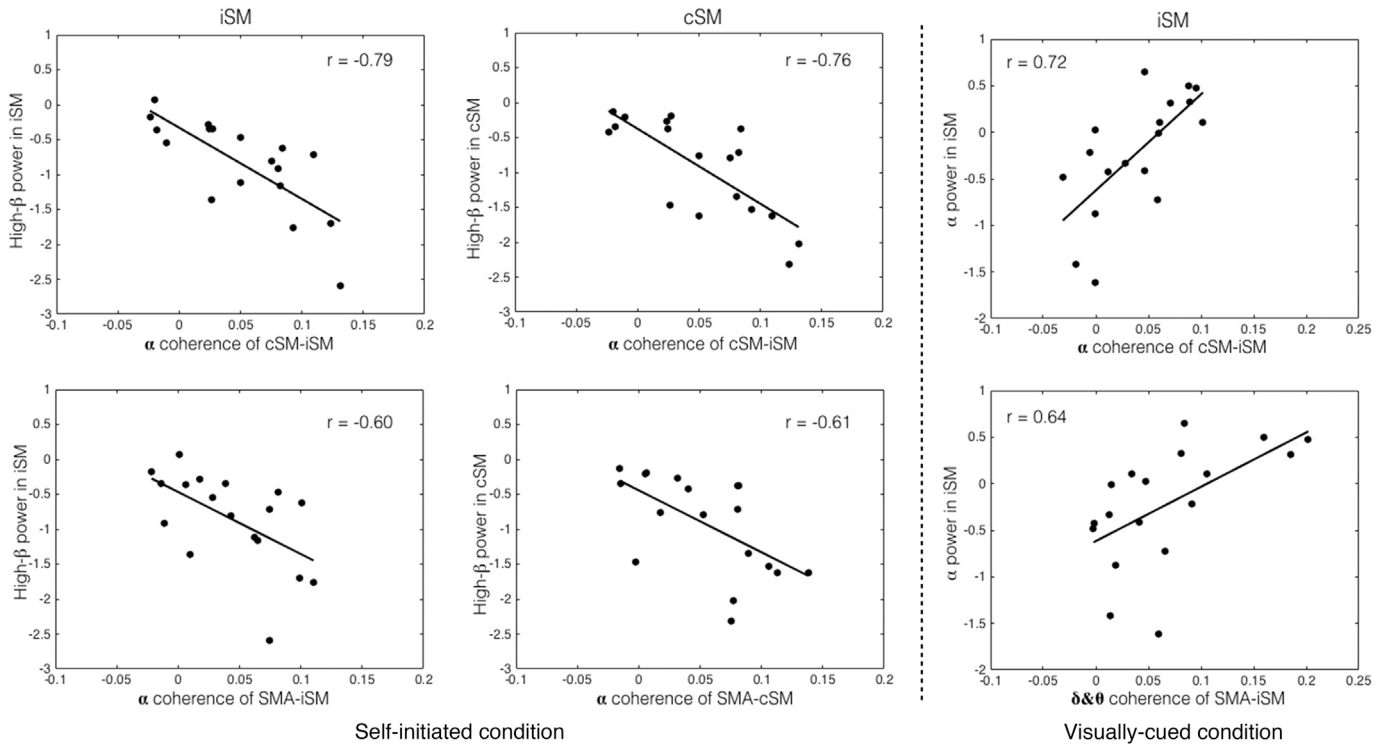

Fig. 7. The Spearman correlation between the averaged coherences of cSM-iSM and SMA-iSM and the averaged powers in SM in the time period [-500, 0] ms in the *Self-initiated* condition (left) and *Visually-cued* condition (right), respectively.

the mean δ-θ coherence of SMA-iSM was positively correlated with ERD over iSM only in the α-band ($r = 0.64$, $p < 0.05/3$, Bonferroni corrected).

These findings provide evidence that ERD over the ipsilateral sensorimotor cortex was sensitive to the movement-initiation context and had a network basis associated with its oscillatory coupling to the contralateral sensorimotor cortex and neural populations in the medial premotor cortex.

4. Discussion

4.1. Regional oscillations in iSM and phase coupling with related regions in the motor system under different initiation contexts

EEG oscillations are characterized by their amplitude and phase. While the former represents the strength of the oscillation (power), the latter represents its timing with regard to a reference point in time. The attenuation of regional power over sensorimotor regions within both the α-band (8–13 Hz) and the β-band (13–30 Hz) during movement preparation and execution has been frequently reported (Meirovitch et al., 2015; Notturno et al., 2014; Pfurtscheller, 1989, 1981; Pfurtscheller et al., 2006), and is assumed to be an indicator of oscillatory aspects of cortical activation. Previous studies have suggested that oscillations in higher frequency bands (i.e., β and γ band) may reflect regional processing while oscillations in low frequencies (i.e., θ and α) may reflect functional interactions between distant cortical regions (Von Stein and Sarnthein, 2000). The functional interaction between different regions has been widely estimated by phase-based coherence, which is an indicator of phase-shifted relations between two EEG signals. Previous studies (Gerloff et al., 1998; Perez and Cohen, 2008) suggested that important aspects of information processing in the human motor system could be based on oscillatory activity of at least two levels, which to some extent can operate independently from each other: (i) regional activation (task-related power) and (ii) phase-based functional coupling in the motor system. In our study, we found a contralateral preponderance of the changes in power in *Visually-cued* movements, whereas in *Self-initiated* movements power changes were more bilateral during motor preparation. However, a reversed pattern was found for the coherence between the medial premotor cortex and sensorimotor cortex. Thus, our data suggest that parts of the motor system may work independently by not only changing the regional oscillatory activity of sensorimotor areas, but also by changing the functional coupling of oscillatory activity between premotor and sensorimotor areas of the two hemispheres.

Moreover, the interaction between regional oscillations and network-like oscillatory couplings also plays an important role in the control of activity-dependent changes in the motor system. For example, the phase coupling of slow oscillations (i.e., θ or α-band) between distant brain areas has been shown to modulate local high frequency powers (i.e., β- or γ-band) (Canolty et al., 2009; Mormann et al., 2005; Osipova et al., 2008; Vukelić et al., 2014). In the motor system, the relationship between coherence and event-related changes in spectral power has been investigated in self-paced simple finger movements (Leocani et al., 1997; Rappelsberger et al., 1994). These studies found that an increase in α coherence between sensorimotor and frontal regions was accompanied by decreases in β power before movement and a greater increase in coherence between the bilateral sensorimotor areas after movement compared to before movement (Leocani et al., 1997; Rappelsberger et al., 1994). However, none of these studies focused on the ipsilateral power changes over sensorimotor cortex and its modulation by different modes of movement initiation.

A number of fMRI and EEG studies showed that ipsilateral motor cortex activations during unilateral hand movements rely on an active and discrete interaction between bilateral sensorimotor areas (Grefkes and Fink, 2011; Kobayashi et al., 2003; B. Van Wijk et al., 2012), although hand dominance may modulate these interactions (Ziemann and Hallett, 2001). A study using transcranial magnetic stimulation (TMS) showed that the amount of interhemispheric inhibition (IHI) from contralateral to ipsilateral primary motor cortex was related to the activity of intracortical GABAergic inhibitory interneurons in ipsilateral primary motor cortex during force generation (Perez and Cohen, 2008).

These data provide evidence that interhemispheric projections influence local inhibitory activity in the primary motor cortex ipsilateral to the moving hand, possibly preventing co-contractions of the "inactive" hand during performance of an unimanual motor task by the other hand (Perez and Cohen, 2008). Using dynamic causal modelling of fMRI activity during simple visually-cued hand movements, we showed earlier that ipsilateral SM activity is suppressed by inhibitory influences originating from contralateral SM (Grefkes et al., 2008a, 2008b). Similarly, previous studies (Obhi and Haggard, 2004; Toni et al., 2001; Waszak et al., 2005) have shown that the medial premotor cortex (SMA) is particularly engaged in self-initiated movements. Furthermore, an increasing number of studies have concluded that the modulation of θ band activity over the medial premotor cortex (represented by the FCz electrode) in externally triggered movements reflects monitoring of actions and error adaption (Cavanagh and Frank, 2014; Cohen and Donner, 2013). Using EEG and Granger analysis, Boenstrup and colleagues also showed increased information flow from the SMA to the ipsilateral motor cortex in the α frequency band during complex finger movements (Boenstrup et al., 2014).

Our results are consistent with these previous studies as they show that the interaction between the ipsilateral sensorimotor cortex and the contralateral sensorimotor cortex as well as the medial premotor cortex is involved in the control of the modulation of ipsilateral oscillations for both movement initiation modes. This might serve the purpose of suppressing output to the muscles of the non-moving hand. Although coherence has been widely adopted in EEG studies as a marker of communication between the signals from two EEG electrodes, it seems possible that an increase in coherence between two neighboring EEG signals may result from an increased input from a tertiary common neural source due to volume conduction (Saltzbertg et al., 1986), particularly for low frequencies. Our use of surface-Laplacian transformation (see Section 2.4.3) reduces but does not entirely eliminate this possibility (Lachaux et al., 1999). Therefore, our results of coherence between the neighboring regions SMA and iSM should be treated with caution as these may result from a common source. Our results on the coherence between the more distant regions cSM and iSM, however, are robust. In our study, we found that *Self-initiated* movements involved bilateral oscillatory power changes over sensorimotor areas and that the participants with stronger coherences between cSM-iSM in the α-band exhibited a larger decrease in high-β power over the sensorimotor cortex. In contrast, a contralateral preponderance of power changes was mainly observed during *Visually-cued* movements and participants with stronger coherence between cSM-iSM in the α-band exhibited less decrease in α power only over the ipsilateral sensorimotor cortex in the *Visually-cued* condition.

4.2. Distinct roles for α and β-band oscillations in different initiation contexts for inhibition in iSM prior to movement

Increases in power of the oscillations in the α-band have been suggested to reflect inhibitory control and timing of cortical processing, whereas decreases in power of α oscillations may reflect a gradual release of inhibition and increased cellular excitability in thalamocortical systems (Klimesch et al., 2007). In externally-triggered actions, our data showed that the changes in interhemispheric interaction between the iSM and cSM were positively correlated with the changes of α power over iSM, albeit not over cSM. Therefore, we suggest that the α power increase over ipsilateral sensorimotor cortex plays a role in ipsilateral inhibition to facilitate the contralateral processing of an upcoming movement. Thus, interhemispheric interactions might subserve the purpose to modulate the extent of this inhibition of the excitation of the ipsilateral sensorimotor cortex. Recently, Brinkman et al. (2014) also demonstrated distinct roles of α and β-band oscillations in a mental simulation of a goal-directed action task. They proposed that an increase in the synchronization of neural oscillations in the α-band in the ipsilateral motor cortex plays a role in disengaging task-irrelevant cortical regions, which is consistent with our results.

Oscillations in the β-band are generally interpreted to reflect regional processing that is related to the control of muscle activity and proprioceptive feedback (Baker, 2007; Jackson et al., 2002). The β desynchronization (ERD) constitutes a reliable indicator of movement preparation in voluntary movements (Meirovitch et al., 2015; Notturno et al., 2014; Pfurtscheller, 1989, 1981; Pfurtscheller et al., 2006). Brinkman et al. (2014) further proposed that the reduction in power of the neural oscillations in the β-band over contralateral sensorimotor cortex is related to the disinhibition of neuronal populations involved in the movement. In our study, we found a dominant bilateral power decrease in the β oscillations, which were modulated by interhemispheric interaction between the iSM and cSM prior to movement onset in the *Self-initiated* condition. Although the functional role of β oscillations remains debated, our results suggest that the decreases in power of the β oscillations are related to the gradual release of inhibition in the motor cortex to initiate an action. The functional relevance of the reduction of β band oscillations for the disinhibition of neuronal populations in the motor system becomes particularly evident under the pathological conditions, e.g. in Parkinson's disease, where high β band activity severely compromises movement initiation and execution (Brown, 2007; Jenkinson and Brown, 2011). Additionally, a higher reduction of β-band activity caused by deep brain stimulation (DBS) leads to an improvement of movement capabilities in patients (Wingeier et al., 2006; Kuhn et al., 2008; Bronte-Stewart et al., 2009). We, therefore, propose that the decrease in β-band power observed in our study is related to the disinhibition of neuronal populations preceding movement execution in order to enable the timely initiation of the internally triggered action (Engel and Fries, 2010; Brinkman et al., 2014). Such a disinhibitory role of β-band power might also apply to the ipsilateral sensorimotor cortex as it has been proposed that hyperactive ipsilateral activity reported in patients with lesions (due to a brain tumor or after a stroke) is partially attributable to interhemispheric disinhibition (Shimizu et al., 2002; Murase et al., 2004; Oshino et al., 2008). This mechanism is different from the ipsilateral inhibitory mechanisms supported by oscillations in the α-band during the externally triggered actions.

Different cortico-subcortical motor processes might be underlying the distinct roles in cortical inhibition by α and β oscillations. Using simultaneous depth and scalp EEG recording, Klostermann et al. (2007) found the decrease in β-band power to be uniform in motor cortical and subcortical recordings (thalamic ventral intermediate nucleus (VIM) or the subthalamic nucleus (STN)) of subjects performing a choice-reaction task with pre-cued Go-signals. However, a comparable decrease in α-band power was only seen at the scalp, whereas an increase in α power was observed in the motor-inhibitory STN. In contrast, Paradiso et al. (2004) found a decrease in thalamic α-band power preceding motor execution in an internally triggered wrist extension task, which suggested a possible differential processing of the preparation of cued vs. self-paced movements with a thalamic role more active in internally than externally-triggered actions. These dissociations of task-related α- and β-band dynamics revealed a functional diversity in cortico-subcortical networks dependent upon how the movement was initiated. This conclusion might extend to our results, but this issue deserves further investigation.

5. Conclusion

In summary, we used EEG to investigate the mechanisms by which the motor system modulates ipsilateral oscillatory activity in the pre-movement period immediately preceding movement onset under the control of two different movement initiating networks. Our findings suggest that the ipsilateral sensorimotor cortex responds not only by changing its state of activation, but also by changing information flow between premotor and contralateral sensorimotor areas. Importantly, the interaction between regional oscillations and network-like oscillatory couplings implies a differential, frequency-specific inhibitory mechanism

in the ipsilateral sensorimotor cortex dependent upon how the movement is initiated.

Conflicts of interest

The authors declare no competing financial interests.

Acknowledgements

This work was funded by the University of Cologne Emerging Groups Initiative (CONNECT group) implemented into the Institutional Strategy of the University of Cologne and the German Excellence Initiative. SD gratefully acknowledges additional support from the German Research Foundation (GR3690/2-1, DA 1953/5-2). GRF gratefully acknowledges additional support from the Marga and Walter Boll Foundation. We are grateful to E. Niessen, I. Weber, P. Loehren, L. Liu for their valuable technical assistance. We particularly thank the two anonymous reviewers for their constructive comments, which helped to improve our manuscript.

Appendix A. Supplementary data

Supplementary data related to this article can be found at http://dx.doi.org/10.1016/j.neuroimage.2017.07.054.

References

Babiloni, C., Brancucci, A., Vecchio, F., Arendt-Nielsen, L., Chen, A.C.N., Rossini, P.M., 2006. Anticipation of somatosensory and motor events increases centro-parietal functional coupling: an EEG coherence study. Clin. Neurophysiol. 117, 1000–1008. http://dx.doi.org/10.1016/j.clinph.2005.12.028.

Bai, O., Mari, Z., Vorbach, S., Hallett, M., 2005. Asymmetric spatiotemporal patterns of event-related desynchronization preceding voluntary sequential finger movements: a high-resolution EEG study. Clin. Neurophysiol. 116, 1213–1221. http://dx.doi.org/10.1016/j.clinph.2005.01.006.

Baker, S.N., 2007. Oscillatory interactions between sensorimotor cortex and the periphery. Curr. Opin. Neurobiol. 17, 649–655. http://dx.doi.org/10.1016/j.conb.2008.01.007.

Boenstrup, M., Feldheim, J., Heise, K., Gerloff, C., Hummel, F.C., 2014. The control of complex finger movements by directional information flow between mesial frontocentral areas and the primary motor cortex. Eur. J. Neurosci. 40, 2888–2897. http://dx.doi.org/10.1111/ejn.12657.

Bronte-Stewart, H., Barberini, C., Koop, M.M., Hill, B.C., Henderson, J.M., Wingeier, B., 2009. The STN beta-band profile in Parkinson's disease is stationary and shows prolonged attenuation after deep brain stimulation, Exp. Neurol 215, 20–28.

Boudrias, M.H., Gonçalves, C.S., Penny, W.D., Park, C.H., Rossiter, H.E., Talelli, P., Ward, N.S., 2012. Age-related changes in causal interactions between cortical motor regions during hand grip. Neuroimage 59, 3398–3405. http://dx.doi.org/10.1016/j.neuroimage.2011.11.025.

Brown, P., 2007. Abnormal oscillatory synchronisation in the motor system leads to impaired movement. Curr. Opin. Neurobiol. 17, 656–664.

Brinkman, L., Stolk, A., Dijkerman, H.C., de Lange, F.P., Toni, I., 2014. Distinct roles for alpha- and beta-band oscillations during mental simulation of goal-directed actions. J. Neurosci. 34, 14783–14792. http://dx.doi.org/10.1523/JNEUROSCI.2039-14.2014.

Canolty, R.T., Edwards, E., Dalal, S.S., Soltani, M., Nagarajan, S.S., Berger, M.S., Barbaro, N.M., Knight, R.T., 2009. High gamma power is phase-locked to theta oscillations in human neocortex. Science 313 (80), 1626–1628. http://dx.doi.org/10.1126/science.1128115.High.

Cavanagh, J.F., Frank, M.J., 2014. Frontal theta as a mechanism for cognitive control. Trends Cogn. Sci. 18, 414–421. http://dx.doi.org/10.1016/j.tics.2014.04.012.

Chen, R., Gerloff, C., Hallett, M., Cohen, L.G., 1997. Involvement of the ipsilateral motor cortex in finger movements of different complexities. Ann. Neurol. 41, 247–254. http://dx.doi.org/10.1002/ana.410410216.

Cincotta, M., Borgheresi, A., Balestrieri, F., Giovannelli, F., Rossi, S., Ragazzoni, A., Zaccara, G., Ziemann, U., 2004. Involvement of the human dorsal premotor cortex in unimanual motor control: an interference approach using transcranial magnetic stimulation. Neurosci. Lett. 367, 189–193. http://dx.doi.org/10.1016/j.neulet.2004.06.003.

Cohen, M.X., 2014. Analyzing Neural Time Series Data: Theory and Practice. MIT Press, Cambridge, MA.

Cohen, M.X., Donner, T.H., 2013. Midfrontal conflict-related theta-band power reflects neural oscillations that predict behavior. J. Neurophysiol. 110, 2752–2763. http://dx.doi.org/10.1152/jn.00479.2013.

Delorme, A., Makeig, S., 2004. EEGLAB: an open source toolbox for analysis of single-trial EEG dynamics including independent component analysis. J. Neurosci. Methods 134, 9–21. http://dx.doi.org/10.1016/j.jneumeth.2003.10.009.

Desmurget, M., Sirigu, A., 2009. A parietal-premotor network for movement intention and motor awareness. Trends Cogn. Sci. 13, 411–419. http://dx.doi.org/10.1016/j.tics.2009.08.001.

Eagleman, D.M., 2004. The where and when of intention. Science 303 (80), 1144–1147.

Engel, A.K., Fries, P., 2010. Beta-band oscillations-signalling the status quo? Curr. Opin. Neurobiol. 20, 156–165. http://dx.doi.org/10.1016/j.conb.2010.02.015.

Gerloff, C., Richard, J., Hadley, J., Schulman, A.E., Honda, M., Hallett, M., 1998. Functional coupling and regional activation of human cortical motor areas during simple, internally paced and externally paced finger movements. Brain 121, 1513–1531. http://dx.doi.org/10.1093/brain/121.8.1513.

Grefkes, C., Eickhoff, S.B., Nowak, D.A., Dafotakis, M., Fink, G.R., 2008a. Dynamic intra- and interhemispheric interactions during unilateral and bilateral hand movements assessed with fMRI and DCM. Neuroimage 41, 1382–1394. http://dx.doi.org/10.1016/j.neuroimage.2008.03.048.

Grefkes, C., Fink, G.R., 2011. Reorganization of cerebral networks after stroke: new insights from neuroimaging with connectivity approaches. Brain 134, 1264–1276. http://dx.doi.org/10.1093/brain/awr033.

Grefkes, C., Nowak, Da, Eickhoff, S.B., Dafotakis, M., Küst, J., Karbe, H., Fink, G.R., 2008b. Cortical connectivity after subcortical stroke assessed with functional magnetic resonance imaging. Ann. Neurol. 63, 236–246. http://dx.doi.org/10.1002/ana.21228.

Haggard, P., 2008. Human volition: towards a neuroscience of will. Nat. Rev. Neurosci. 9, 934–946. http://dx.doi.org/10.1038/nrn2497.

Herwig, A., Prinz, W., Waszak, F., 2007. Two modes of sensorimotor integration in intention-based and stimulus-based actions. Q. J. Exp. Psychol. (Hove) 60, 1540–1554. http://dx.doi.org/10.1080/17470210601119134.

Hsieh, J.-C., Cheng, H., Hsieh, H.-M., Liao, K.-K., Wu, Y.-T., Yeh, T.-C., Ho, L.-T., 2002. Loss of interhemispheric inhibition on the ipsilateral primary sensorimotor cortex in patients with brachial plexus injury: fMRI study. Ann. Neurol. 51, 381–385.

Hummel, F., Kirsammer, R., Gerloff, C., 2003. Ipsilateral cortical activation during finger sequences of increasing complexity: representation of movement difficulty or memory load? Clin. Neurophysiol. 114, 605–613. http://dx.doi.org/10.1016/S1388-2457(02)00417-0.

Jackson, a, Spinks, R.L., Freeman, T.C.B., Wolpert, D.M., Lemon, R.N., 2002. Rhythm generation in monkey motor cortex explored using pyramidal tract stimulation. J. Physiol. 541, 685–699. http://dx.doi.org/10.1113/jphysiol.2001.015099.

Jenkinson, N., Brown, P., 2011. New insights into the relationship between dopamine, beta oscillations and motor function. Trends Neurosci 34, 611–618.

Jahanshahi, M., Jenkins, H., Brown, R., Marsden, C., Passingham, R., Brooks, D., 1995. Self-initiated versus Externally Triggered Movements .1. An Investigation Using Measurement of Regional Cerebral Blood-flow with Pet and Movement-related Potentials in Normal and Parkinsons-disease Subjects, pp. 913–933.

Kayser, J., Tenke, C.E., 2006. Principal components analysis of Laplacian waveforms as a generic method for identifying ERP generator patterns: II. Adequacy of low-density estimates. Clin. Neurophysiol. 117, 369–380. http://dx.doi.org/10.1016/j.clinph.2005.08.033.

Keil, A., Elbert, T., Taub, E., 1999. Relation of accelerometer and EMG recordings for the measurement of upper extremity movement. J. Psychophysiol. 13, 77–82. http://dx.doi.org/10.1027//0269-8803.13.2.77.

Klimesch, W., Sauseng, P., Hanslmayr, S., 2007. EEG alpha oscillations: the inhibition-timing hypothesis. Brain Res. Rev. 53, 63–88. http://dx.doi.org/10.1016/j.brainresrev.2006.06.003.

Klostermann, F., Nikulin, V.V., Kühn, A.A., Marzinzik, F., Wahl, M., Pogosyan, A., Kupsch, A., Schneider, G.H., Brown, P., Curio, G., 2007. Task-related differential dynamics of EEG alpha- and beta-band synchronization in cortico-basal motor structures. Eur. J. Neurosci. 25, 1604–1615. http://dx.doi.org/10.1111/j.1460-9568.2007.05417.x.

Kobayashi, M., Hutchinson, S., Schlaug, G., Pascual-Leone, A., 2003. Ipsilateral motor cortex activation on functional magnetic resonance imaging during unilateral hand movements is related to interhemispheric interactions. Neuroimage 20, 2259–2270. http://dx.doi.org/10.1016/S1053-8119(03)00220-9.

Kuhn, A.A., Kempf, F., Brucke, C., Gaynor Doyle, L., Martinez-Torres, I., Pogosyan, A., Trottenberg, T., Kupsch, A., Schneider, G.-H., Hariz, M.I., Vandenberghe, W., Nuttin, B., Brown, P., 2008. High-frequency stimulation of the subthalamic nucleus suppresses oscillatory activity in patients with Parkinson's disease in parallel with improvement in motor performance. J. Neurosci 28, 6165–6173.

Krieghoff, V., Waszak, F., Prinz, W., Brass, M., 2011. Neural and behavioral correlates of intentional actions. Neuropsychologia 49, 767–776. http://dx.doi.org/10.1016/j.neuropsychologia.2011.01.025.

Lachaux, J., Rodriguez, E., Martinerie, J., Varela, F.J., 1999. Measuring Phase Synchrony in Brain signals.Pdf, vol. 208, pp. 194–208.

Leocani, L., Toro, C., Manganotti, P., Zhuang, P., Hallett, M., 1997. Event-related coherence and event-related desynchronization/synchronization in the 10 Hz and 20 Hz EEG during self- paced movements. Electroencephalogr. Clin. Neurophysiol. - Evoked Potentials 104, 199–206. http://dx.doi.org/10.1016/S0168-5597(96)96051-7.

Makeig, S., 1993. Auditory event-related dynamics of the EEG spectrum and effects of exposure to tones. Electroencephalogr. Clin. Neurophysiol. 86, 283–293. http://dx.doi.org/10.1016/0013-4694(93)90110-H.

Manganotti, P., Gerloff, C., Toro, C., Katsuta, H., Sadato, N., Zhuang, P., Leocani, L., Hallett, M., 1998. Task-related coherence and task-related spectral power changes during sequential finger movements. Electroencephalogr. Clin. Neurophysiol. - Electromyogr. Mot. Control 109, 50–62. http://dx.doi.org/10.1016/S0924-980X(97)00074-X.

Meirovitch, Y., Harris, H., Dayan, E., Arieli, A., Flash, T., 2015. Alpha and beta band event-related desynchronization reflects kinematic regularities. J. Neurosci. 35, 1627–1637. http://dx.doi.org/10.1523/JNEUROSCI.5371-13.2015.

Michely, J., Barbe, M.T., Hoffstaedter, F., Timmermann, L., Eickhoff, S.B., Fink, G.R., Grefkes, C., 2012. Differential effects of dopaminergic medication on basic motor performance and executive functions in Parkinson's disease. Neuropsychologia 50, 2506–2514. http://dx.doi.org/10.1016/j.neuropsychologia.2012.06.023.

Michely, J., Volz, L.J., Barbe, M.T., Hoffstaedter, F., Viswanathan, S., Timmermann, L., Eickhoff, S.B., Fink, G.R., Grefkes, C., 2015. Dopaminergic modulation of motor network dynamics in Parkinson's disease. Brain 1–15. http://dx.doi.org/10.1093/brain/awu381.

Mognon, A., Jovicich, J., Bruzzone, L., Buiatti, M., 2011. ADJUST: an automatic EEG artifact detector based on the joint use of spatial and temporal features. Psychophysiology 48, 229–240. http://dx.doi.org/10.1111/j.1469-8986.2010.01061.x.

Mormann, F., Fell, J., Axmacher, N., Weber, B., Lehnertz, K., Elger, C.E., Fernández, G., 2005. Phase/amplitude reset and theta-gamma interaction in the human medial temporal lobe during a continuous word recognition memory task. Hippocampus 15, 890–900. http://dx.doi.org/10.1002/hipo.20117.

Murase, N., Duque, J., Mazzocchio, R., Cohen, L.G., 2004. Influence of interhemispheric interactions on motor function in chronic stroke. Ann. Neurol 55, 400–409.

Mueller, Va, Brass, M., Waszak, F., Prinz, W., 2007. The role of the preSMA and the rostral cingulate zone in internally selected actions. Neuroimage 37, 1354–1361. http://dx.doi.org/10.1016/j.neuroimage.2007.06.018.

Notturno, F., Marzetti, L., Pizzella, V., Uncini, A., Zappasodi, F., 2014. Local and remote effects of transcranial direct current stimulation on the electrical activity of the motor cortical network. Hum. Brain Mapp. 35, 2220–2232. http://dx.doi.org/10.1002/hbm.22322.

Obhi, S.S., Haggard, P., 2004. Internally generated and externally triggered actions are physically distinct and independently controlled. Exp. Brain Res. 156, 518–523. http://dx.doi.org/10.1007/s00221-004-1911-4.

Oldfield, 1971. The assessment and analysis of handedness: the Edinburgh inventory. Neuropsychologia 9, 97–113.

Oshino, S., Kato, A., Hirata, M., Kishima, H., Saitoh, Y., Fujinaka, T., Yoshimine, T., 2008. Ipsilateral motor-related hyperactivity in patients with cerebral occlusive vascular disease. Stroke 39, 2769–2775.

Osipova, D., Hermes, D., Jensen, O., 2008. Gamma power is phase-locked to posterior alpha activity. PLoS One 3, 1–7. http://dx.doi.org/10.1371/journal.pone.0003990.

Paradiso, G., Cunic, D., Saint-Cyr, J.A., Hoque, T., Lozano, A.M., Lang, A.E., Chen, R., 2004. Involvement of human thalamus in the preparation of self-paced movement. Brain 127, 2717–2731. http://dx.doi.org/10.1093/brain/awh288.

Perez, Ma, Cohen, L.G., 2008. Mechanisms underlying functional changes in the primary motor cortex ipsilateral to an active hand. J. Neurosci. 28, 5631–5640. http://dx.doi.org/10.1523/JNEUROSCI.0093-08.2008.

Perrin, F., Pernier, J., Bertrand, O., Echallier, J.F., 1989. Spherical splines for scalp potential and current density mapping. Electroencephalogr. Clin. Neurophysiol. 72, 184–187. http://dx.doi.org/10.1016/0013-4694(89)90180-6.

Pfurtscheller, G., 1989. Functional topography during sensorimotor activation studied with event-related desynchronization mapping. J. Clin. Neurophysiol. http://dx.doi.org/10.1097/00004691-198901000-00003.

Pfurtscheller, G., 1981. Central beta rhythm during sensorimotor activities in man. Electroencephalogr. Clin. Neurophysiol. 51, 253–264. http://dx.doi.org/10.1016/0013-4694(81)90139-5.

Pfurtscheller, G., Brunner, C., Schlögl, a., Lopes da Silva, F.H., 2006. Mu rhythm (de) synchronization and EEG single-trial classification of different motor imagery tasks. Neuroimage 31, 153–159. http://dx.doi.org/10.1016/j.neuroimage.2005.12.003.

Pfurtscheller, G., Lopes Da Silva, F.H., 1999. Event-related EEG/MEG synchronization and desynchronization: basic principles. Clin. Neurophysiol. 110, 1842–1857. http://dx.doi.org/10.1016/S1388-2457(99)00141-8.

Popovych, S., Rosjat, N., Toth, T.I., Wang, Ba, Liu, L., Abdollahi, R.O., Viswanathan, S., Grefkes, C., Fink, G.R., Daun, S., 2016. Movement-related phase locking in the delta–theta frequency band. Neuroimage 139, 439–449. http://dx.doi.org/10.1016/j.neuroimage.2016.06.052.

Rappelsberger, P., Pfurtscheller, G., Filz, O., 1994. Calculation of event-related coherence–a new method to study short-lasting coupling between brain areas. Brain Topogr. 7, 121–127. http://dx.doi.org/10.1007/bf01186770.

Rigoni, D., Brass, M., Roger, C., Vidal, F., Sartori, G., 2013. Top-down modulation of brain activity underlying intentional action and its relationship with awareness of intention: an ERP/Laplacian analysis. Exp. Brain Res. 229, 347–357. http://dx.doi.org/10.1007/s00221-013-3400-0.

Rossiter, H.E., Davis, E.M., Clark, E.V., Boudrias, M.H., Ward, N.S., 2014. Beta oscillations reflect changes in motor cortex inhibition in healthy ageing. Neuroimage 91, 360–365. http://dx.doi.org/10.1016/j.neuroimage.2014.01.012.

Saltzberg, B., Burton, W.D., Burch, N.R., Fletcher, J., Michaels, R., 1986. Electrophysiological measures of regional neural interactive coupling. Linear and non-linear dependence relationships among multiple channel electroencephalographic recordings. Int. J. Biomed. Comput. 18, 77–87. http://dx.doi.org/10.1016/0020-7101(86)90050-4.

Steinmetz, H., Furst, G., Meyer, B.U., 1989. Craniocerebral topography within the international 10-20 system. Electroencephalogr. Clin. Neurophysiol. 72, 499–506.

Steogonpień, M., Conradi, J., Waterstraat, G., Hohlefeld, F.U., Curio, G., Nikulin, V.V., 2011. Event-related desynchronization of sensorimotor EEG rhythms in hemiparetic patients with acute stroke. Neurosci. Lett. 488, 17–21. http://dx.doi.org/10.1016/j.neulet.2010.10.072.

Shimizu, T., Hosaki, A., Hino, T., Sato, M., Komori, T., Hirai, S., Rossini, P.M., 2002. Motor cortical disinhibition in the unaffected hemisphere after unilateral cortical stroke. Brain 125, 1896–1907.

Storti, S.F., Formaggio, E., Manganotti, P., Menegaz, G., 2015. Brain network connectivity and topological analysis during voluntary arm movements. Clin. EEG Neurosci. http://dx.doi.org/10.1177/1550059415598905.

Szurhaj, W., Labyt, E., Bourriez, J.L., Cassim, F., Defebvre, L., Hauser, J.J., Guieu, J.D., Derambure, P., 2001. Event-related variations in the activity of EEG-rhythms. Application to the physiology and the pathology of movements. Epileptic Disord. Spec. Issue 59–66.

Tangwiriyasakul, C., Verhagen, R., Rutten, W.L.C., van Putten, M.Ja M., 2013. Temporal evolution of event-related desynchronization in acute stroke: a pilot study. Clin. Neurophysiol. 125, 1112–1120. http://dx.doi.org/10.1016/j.clinph.2013.10.047.

Tenke, C.E., Kayser, J., Manna, C.G., Fekri, S., Kroppmann, C.J., Schaller, J.D., Alschuler, D.M., Stewart, J.W., Mcgrath, P.J., Bruder, G.E., 2012. Current source density measures of EEG alpha predict antidepressant treatment response. Biol. Psychiatry 70, 388–394. http://dx.doi.org/10.1016/j.biopsych.2011.02.016.Current.

Tinazzi, M., Zanette, G., 1998. Modulation of ipsilateral motor cortex in man during unimanual finger movements of different complexities. Neurosci. Lett. 244, 121–124. http://dx.doi.org/10.1016/S0304-3940(98)00150-5.

Toni, I., Rushworth, M.F.S., Passingham, R.E., 2001. Neural correlates of visuomotor associations spatial rules compared with arbitrary rules. Exp. Brain Res. 141, 359–369. http://dx.doi.org/10.1007/s002210100877.

Van Wijk, B., Beek, P., Daffertshofer, A., 2012a. Differential modulations of ipsilateral and contralateral beta (de)synchronization during unimanual force production. Eur. J. Neurosci. 36, 2088–2097. http://dx.doi.org/10.1111/j.1460-9568.2012.08122.x.

Verleger, R., Adam, S., Rose, M., Vollmer, C., Wauschkuhn, B., Kömpf, D., 2003. Control of hand movements after striatocapsular stroke: high-resolution temporal analysis of the function of ipsilateral activation. Clin. Neurophysiol. 114, 1468–1476. http://dx.doi.org/10.1016/S1388-2457(03)00125-1.

Von Stein, A., Sarnthein, J., 2000. Different frequencies for different scales of cortical integration: from local gamma to long range alpha/theta synchronization. Int. J. Psychophysiol. 38, 301–313. http://dx.doi.org/10.1016/S0167-8760(00)00172-0.

Vukelić, M., Bauer, R., Naros, G., Naros, I., Braun, C., Gharabaghi, A., 2014. Lateralized alpha-band cortical networks regulate volitional modulation of beta-band sensorimotor oscillations. Neuroimage 87, 147–153. http://dx.doi.org/10.1016/j.neuroimage.2013.10.003.

Ward, N.S., Swayne, O.B.C., Newton, J.M., 2008. Age-dependent changes in the neural correlates of force modulation: an fMRI study. Neurobiol. Aging 29, 1434–1446. http://dx.doi.org/10.1016/j.neurobiolaging.2007.04.017.

Wingeier, B., Tcheng, T., Koop, M.M., Hill, B.C., Heit, G., Bronte-Stewart, H.M., 2006. Intra-operative STN DBS attenuates the prominent beta rhythm in the STN in Parkinson's disease. Exp. Neurol 197, 244–251.

Waszak, F., Wascher, E., Keller, P., Koch, I., Aschersleben, G., Rosenbaum, Da, Prinz, W., 2005. Intention-based and stimulus-based mechanisms in action selection. Exp. Brain Res. 162, 346–356. http://dx.doi.org/10.1007/s00221-004-2183-8.

Ziemann, U., Hallett, M., 2001. Hemispheric asymmetry of ipsilateral motor cortex activation during unimanual motor tasks: further evidence for motor dominance. Clin. Neurophysiol. 112, 107–113.

Zimerman, M., Heise, K.F., Gerloff, C., Cohen, L.G., Hummel, F.C., 2014. Disrupting the ipsilateral motor cortex interferes with training of a complex motor task in older adults. Cereb. Cortex 24, 1030–1036. http://dx.doi.org/10.1093/cercor/bhs385.